EFDA–JET–PR(10)33

A. Murari, D. Mazon, A. Debrie
and JET EFDA contributors

On the Use of Non-Additive Entropy to Determine the Presence of Vibrations in the Videos of JET Cameras

On the Use of Non-Additive Entropy to Determine the Presence of Vibrations in the Videos of JET Cameras

A. Murari[1], D. Mazon[2], A. Debrie[3]
and JET EFDA contributors*

JET-EFDA, Culham Science Centre, OX14 3DB, Abingdon, UK

[1]Associazione EURATOM-ENEA per la Fusione, Consorzio RFX, 4-35127 Padova, Italy
[2]Association EURATOM-CEA, CEA Cadarache, 13108 Saint-Paul-lez-Durance, France
[3]Arts et Métiers ParisTech Engineering College (ENSAM) 75013 Paris.
** See annex of F. Romanelli et al, "Overview of JET Results",*
(23rd IAEA Fusion Energy Conference, Daejon, Republic of Korea (2010)).

Preprint of Paper to be submitted for publication in
Pattern Recognition

ABSTRACT

In many domains where images are produced and acquired, the field of view of cameras can be subject to oscillations and movements, which can induce errors in the interpretation of the frame contents and can even jeopardise the analysis of the videos. The problem is particularly severe in applications, such as Nuclear Fusion, in which typically no stable and reliable reference points exist within the camera fields of view to register the frames. A non-additive form of entropy Sq, which is more sensitive than the Shannon entropy to long range correlations, has been applied to the problem of automatically detecting such camera movements in the videos of JET wide angle infrared camera. A systematic analysis of the results, covering more than 110,000 frames, has been undertaken and the results obtained, reaching a total success rate of almost 97%, are more than satisfactory.

1. INTRODUCTION

The digital universe is expanding at a very high rate. The amount of data generated in the world increases of a factor of 10 in less than every 5 years [1]. In 2007 it has been estimated that about 281 exabytes of new data were generated. Of this data deluge, images are taken progressively the lion's share. The increased resolution of digital cameras, the growth of surveillance and the spread of camera phones are the main factors driving this trend. In general nowadays the media, broadcast and entertainment industries already generate and manage about 50% of the digital universe exactly for the reason that they mainly handle images.

The data deluge is being clearly perceived also in the scientific community and again one of the main drivers is the increased penetration of cameras in the world of instrumentation. For example, many more cameras, both visible and infrared, have become routine diagnostics in Magnetic Confinement Nuclear Fusion (MCNF) in the last years. The Join European Torus has already a global database of more than 90 terabytes of data of which about 50% are images [2,3].

The efficient analysis of such big amounts of images requires the development of quite sophisticated processing tools. In MCNF various innovative solutions have been developed recently for informational retrieval in big repositories of images [4] and for the automatic analysis identification of objects within images [5,6]. New technologies, such as Cellular Nonlinear Networks and FPGA based oriented acquisition systems, have also been successfully upgraded and applied [7,8].

Image processing in MCNF presents some specific challenges, linked to the environment in which the cameras have to work and to the physical objects, thermonuclear plasmas, to be studied. First of all a great variety of objects, from hot spots on the first wall and arcs on various antennas to flying particles, from ablation clouds of pellets to blobs and radiative instabilities, have to be detected and properly identified on a quite fast time scales, sometimes of the order of fractions of a ms [5]. The task is complicated by the changing nature of the background. Indeed a series of instabilities, called Edge Localised Modes (ELMs), tend to completely alter the background illumination at very high frequencies (up to hundreds of Hz) [9].

One of the difficulties affecting various aspects of the image analysis process in MCNF is the presence of strong vibrations of the endoscopes and structures on which the cameras are installed

(see section 4.1 for more details). The movements of the field of view can affect the interpretation of the images and should be identified and corrected both for offline analysis and real time control purposes. The causes of such vibrations are multiple, from ELM instabilities to disruptions, and are also unavoidable. Given the frequency and the entity of the variations in the background illumination, no reliable reference points are present in the frames to readjust the videos and therefore an original approach is required to both detect and re-centre the frames affected by vibrations. The main idea behind the developed method is based on the properties of the differences between two subsequent frames. If the camera field of view remains stable and only objects move inside the frame, the difference between subsequent frames contains structures, which present quite short range correlations. On the other hand, in the case a global movement of the field of view has occurred between two frames, the difference typically exhibits structures with much longer correlation lengths. These observations can be put on sound mathematical basis using an alternative, non-additive definition of entropy also called Tsallis entropy [10], indicated by the symbol Sq. As described in more details in the next two sections, the non-additive entropy Sq is particularly well suited to extracting these long range correlations from the two dimensional images obtained by the difference of subsequent experimental frames. Sq therefore results a very powerful tool to detect movements of the field of view for cameras in which no obvious and reliable reference points are present.

With regard to the structure of the paper, the mathematical properties of the Sq entropy are presented in the next section. The main rational behind its application to images to detect vibrations is the subject of section 3, in which some numerical simple examples are presented. In section 4 the proposed approach is applied to a large database of JET videos (70 videos and more than 110,000 frames) and the success rate is discussed. Conclusions and the lines of future investigations are the subject of the last section 5.

2. THE NON ADDITIVE SQ ENTROPY AND ITS MAIN PROPERTIES

Originally entropy is a basic thermodynamic concept that is associated with the evolution of irreversible processes in the universe. In information theory, entropy is a measure of the uncertainty associated to a random variable. In this context, the term usually refers to the Shannon entropy, which quantifies, in the sense of the expected value, the information contained in a message, usually in units such as bits. The concept was introduced by Claude E. Shannon in his 1948 paper "A Mathematical Theory of Communication" [11].

The Shannon entropy can be expressed as:

(1)

Where pi is the probability of finding the system in each possible state i and k is the total number of states. In the case of images, as in the present paper, pi is typically the probability of the pixels having a certain intensity (see section 4.3 for the details).

In 1988, Constantino Tsallis introduced the Sq entropy in his seminal paper [10]. The Sq entropy

generalizes the Shannon entropy to non-additive systems and adds a free parameter q which characterizes the degree of non-additivity.

The Sq entropy is defined as:

(2)

where q is a free parameter, which has to be optimized for each individual application, and k is some conventional positive constant (the Boltzmann constant in the case of traditional Boltzmann-Gibbs statistics). This expression recovers the Shannon entropy in the limit $q \rightarrow 1$ [12]. The Sq entropy shares some properties, such as non-negativity, with the Shannon entropy [12]. On the other hand, one of the main differences with respect to the Shannon entropy is the fact that Sq is non additive since $S_q(A+B) = S_q(A) + S_q(B) + (1-q)\, S_q(A)\, S_q(B)$.

One of the main reasons for the introduction of Sq is the modeling of systems with long term correlations. Sq is well suited to this goal because different values of the free parameters q alter the relative importance of the various probabilities. For example, a q much less than 1 tends to emphasize the role of the lower probabilities. In our application, the free parameter q will be chosen to maximize the chances of properly detecting the movements of the camera field of view. Indeed, selecting a small value for the parameter q, the Sq entropy becomes much more sensitive than traditional Shannon entropy to long range correlations (see sections 3 and 4).

3. APPLICATION TO THE PROBLEMS OF IDENTIFYING VIBRATIONS IN VIDEO FRAMES

In order to illustrate the role of the Sq entropy in our application, a synthetic case is introduced and discussed in this section. Two matrixes of numbers, simulating the pixels of an image, are generated first:

- A 9×9 matrix called “Background Matrix”, which simulates the background seen by the camera.
- A 3×2 matrix called “Object Matrix”, which simulates an object which appears inside the field of view of the camera.

The two matrixes are shown in figure 1; the numerical value in each small square represents the intensity measured by the pixel. It is worth mentioning that the relative dimensions of the two matrixes are representative of the biggest objects which can move inside the images recorded by JET cameras.

Two different combinations of the matrixes are considered (see figure 2):

- The Object and Background matrix are in the field of view and the Object matrix moves.
- The Object and Background matrix are in the field of view and the Background matrix moves.

For each of the two cases, the differences between the two frames are taken and the Sq entropy is calculated for these differences, selecting a value of 0.1 for the q parameter.

As shown in figure 2, the S_q entropy of the background movement is 0,83 higher than the S_q entropy of the object movement. On the contrary, the Shannon entropy of the background movement is only 0,27 higher than the Shannon entropy of the object movement. Even these very simplified examples show very clearly that the S_q entropy is much more sensitive than the traditional Shannon entropy to movements of the background, giving rise long range correlations in the difference of subsequent frames.

4. RESULTS FOR A COMPREHENSIVE DATABASE OF JET VIDEOS

In this section we first introduce the camera, whose videos are used to exemplify the potential of the Sq entropy to detect vibrations. (subsection 4.1). The database of videos, on which the investigation is based, is described in subsection 4.2. The results of the performed statistical analysis are reportd in subsection 4.3.

4.1 INTRODUCTION TO JET CAMERAS

The wide angle cameras in JET have been installed to survey the entire Tokamak cross-section both in the visible and the infrared range of wavelengths. The present study will use the videos acquired by the InfraRed (IR) camera KL7, which is located on an endoscope in Octant 8 and provides a view of Octant 1 and 2 [13]. The endoscope implements a Cassegrain relay optics system and allows a wide angle view of the inside of the vacuum vessel, even if the camera is located at a certain distance from the machine for better shielding (see figure 3). Several structures are included in the endoscope field of view: the ITER-Like Antenna (ILA), the ICRH antenna A and half of the ICRH antenna B. The upper dump plate and most of the divertor are also seen.

The wide angle IR camera was installed on JET in September 2005 and its measurements are of great interest because they show in a very immediate way how Plasma Facing Components (PFC) heat up during a pulse. Normally the live display from the camera is fed through to the left hand monitor above the session leader's desk. The wide angle infrared camera is a digital camera that allows the user to set Regions Of Interest (ROIs). Hence the display might just show a letterbox view. Smaller ROIs allow the camera to capture at faster speeds. Note that the camera has two separate output channels: the live video and the digital channel. Only the video channel is available in real time and it is the one used for the investigations presented in this paper. For precision sake, it is worth mentioning that in the paper the generic term camera movement is used. This is in the interest of simplicity and readability of the paper, because in reality the movements of the field of view of the wide angle IR camera can be due also to oscillations or bending of the entire endoscope. This distinction is immaterial to the objective of the present paper, which is simply aimed at describing a method to automatically identify movements of fields of view independently from the physical origins of these movements. In the following therefore the generic expression camera movement is retained without further qualification.

4.2 INTRODUCTION TO JET DATABASE

In order to obtain general results, 70 shots have been selected covering the vast majority of JET operational space. They include discharges with plasma current between 2 and 3.5MA (Pulse No's:

72822 and 73847 respectively) and toroidal field between 1.9 and 3.4T (Pulse No's: 72822 and 73205 respectively). The selected videos have been taken for a great variety of plasma scenarios and plasma shapes and therefore the results, reported in the following, are considered representative of JET entire operational space.

Given the fact that h eused database is very comprehensive, the selected videos show all the major typical events which can be detected by cameras in JET:

- ELMs (Edge localized modes) which can cause the sudden loss of up to 10–15% of the plasma stored energy. They affect both visible and infrared cameras by creating powerful flashes of light and heat up the divertor (see figure 5a).
- MARFEs (Multifaceted Asymmetric Radiation From the Edge) [14] which are radiative instabilities which generate some of the biggest objects moving inside the field of view of JET cameras (see figure 5b).
- UFOs (Unidentified flying object) which are particles and flakes extracted from the wall by particularly violent plasma wall interactions (see figure 5c).
- Strike point sweeps: Plasma movements which result from the displacement of the strike points in the divertor (to reduce the thermal loads on the divertor tiles)

Practically each frame, of the 113,209 forming the 70 videos, has been analyzed manually, using video editing software, in order to characterize precisely whether the camera has moved during the discharge. An example is shown in figure 6 where two subsequent frames and their difference are shown for a case with and one without vibrations. The appearance of long range structures, due to movements in the background, is very clear in the case of vibrations of the camera's field of view.

4.3 STATISTICAL RESULTS

For each video, the evolution of the Sq entropy can be calculated once the probabilities pi of the pixel intensities have been determined. In our case, since the real time images have pixels which assume 256 different values, it has been decided to divide also the range of probabilities in 256 intervals. An example of the obtained results is reported in figure 7, which shows the evolution of the Sq entropy of the difference between subsequent frames as a function of the frame number. To automatically detect the frames between which a movement of the camera has occurred, a threshold in the Sq entropy has to be found. A systematic analysis has allowed determining that the best value, to discriminate couples of subsequent frames with and without vibrations, is a S_q value of 20.

In terms of classification results, the typical four situations described in the following can arise:

- Frames where no movement is rightly detected: the S_q entropy is lower than the threshold.
- Frames where a movement is rightly detected : the S_q entropy is higher than the threshold.
- False Positives. Frames where a movement is wrongly detected since the S_q entropy is higher than the threshold but there is no movement of the camera's field of view.
- False Negatives. Frames where a movement is not detected since the S_q entropy is lower than the threshold but the camera has moved between the two frames.

Figure 8 shows the result of the overall analysis. The performed systematic analysis of the raw videos shows that the S_q entropy allows determining the presence of vibrations in the wide angle IR camera movies with a success rate of 95.73%. The biggest sources of error are the strong changes in the background illumination caused by ELMs, which result in almost 3% of false alarms. On the contrary the percentage of missed alarms is quite low, 1.37%, particularly considering that the manual classification has always been considered correct, even in the equivocal cases, in which the movements are very small and their real occurrence questionable The obtained success rate is therefore more than satisfactory, also considering the fact that the quality of the video output of the wide angle IR camera is not very high, since the system was originally designed to provide good digital videos for off-line analysis.

In any case in order to reduce the incidence of the false alarms due to ELMs, the historical evolution of the videos has been taken into account. In particular, if at the frame number t, the $S_q$entropy is higher than the threshold value but the S_q entropies of frame number t-1 and t+1 are lower, then it is assumed that the increase of S_q is due to a change in the background illumination. Indeed normally the movements of the camera field of view are due to mechanical vibrations of the supporting endoscope (see subsection 4.1), which are damped on a time scale much longer than the interval between two subsequent frames. Thanks to this simple post processing, 1188 more frames are rightly detected. This results in an improvement of the success rate of 1.05%, allowing to reach a total success rate of almost 97%. The final statistics including this simple post processing method is shown in figure 9.

CONCLUSIONS AND DIRECTIONS OF FURTHER RESEARCH

In this paper an automatic technique to detect movements in the field of view of cameras has been described. The method has been conceived for videos in which no reliable reference points are available within the images to adjust the frames. The implemented solution consists of calculating the S_q entropy of the difference between subsequent frames. When the value of the S_q entropy exceeds a certain value, 20 for the case of JET camera presented in this paper, the probability that a movement occurred between the two frames is very high. With this approach almost 97% success rate has been achieved for a wide database of JET videos covering almost the whole JET operational space and including 113,209 frames. It is worth mentioning that, if the Shannon entropy is used instead of S_q, it has not been possible to obtain a total success rate of 93%.

Even if the results are more than satisfactory for JET applications, further refinements are being considered to improve the success rate even further. Indeed the results presented in the paper have been obtained without any form of preprocessing of the images. On the other hand an equalization of the pixels would probably be advantageous. Since now the video output of JET wired angle camera is compressed to a range of 256 gray levels but originally the scale is of 3000 different values, an equalization of the pixels intensities to the original range would allow a better resolution. Moreover, the most intense pixels, which are typically due to ELMs, could be eliminated hopefully reducing

the number of false positives. Another approach could consist of masking certain regions, such as the divertor, which typically do not provide a lot of information about the movements of the field of view and can even be misleading (like in the case of the sweeping the strike point positions).

Another future line of research will address the implementation of the proposed algorithms in real time. The method has been originally conceived for off line analysis but the results are so encouraging that the deployment in real time for control purposes can be envisaged. The main issue for real time applications is of course the computational time, which has to be short and predictable. To this end the mathematical approach of Cellular Nonlinear Networks is being considered, given the excellent results obtained in other applications [7].

ACKNOWLEDGMENTS

This work was supported by EURATOM and carried out within the framework of the European Fusion Development Agreement. The views and opinions expressed herein do not necessarily reflect those of the European Commission.

REFERENCES

[1]. e-IRG Blue Paper 2010 http://www.alphagalileo.org/AssetViewer

[2]. R. Layne et al Fusion Engineering and Design, Volume **85**, Issues 3-4, July 2010, Pages 403-409

[3]. R. Layne et al, Fusion Engineering and Design, Volume **60**, Issue 3, June 2002, Pages 333-339

[4]. J. Vega et al., Review of Scientific Instruments **79**, 10F327 (2008)

[5]. A. Murari, M. Camplani, B. Cannas, D. Mazon, F. Delaunay, P. Usai, and J.F. Delmond "Algorithms for the Automatic Identification of MARFEs and UFOs in JET Database of Visible Camera Videos" accepted for publication in IEEE Transactions on Plasma Science

[6]. V. Martin IEEE Transactions on instrumentation and Measurement Vol **59**, N° 5, May 2010.

[7]. S. Palazzo et al., Review of Scientific Instruments **81**, 083505 (2010)

[8]. V. Martin Proceeding of HTPD 2010 published in RSI oct 2010].

[9]. J. Wesson "Tokamaks" Clarendon Press, Oxford, third edition, 2004

[10]. C. Tsallis, Possible generalization of Boltzmann-Gibbs statistics, Journal of Statistical Physics **52** (1988) 479–487.

[11]. C.E. Shannon, "A mathematical theory of communication," Bell System Technical Journal, vol. **27**, pp. 379-423 and 623-656, July and October, 1948.

[12]. Constantino Tsallis, "Introduction to nonextensive statistical mechanics" Springer Science + Business Media, Rio de Janeiro, Brazil, 2009

[13]. E. Gauthier et al., Fusion Engineering and Design, **82**(5-14):1335-1340, 2007

[14]. H.B. Lipschultz, B. LaBombard, E.S. Marmar et al., Nuclear Fusion **24** (1984) 977

Background matrix

1	2	3	4	5	6	7	8	9
2	3	4	5	6	7	8	9	1
3	4	5	6	7	8	9	1	2
4	5	6	7	8	9	1	2	3
5	6	7	8	9	1	2	3	4
6	7	8	9	1	2	3	4	5
7	8	9	1	2	3	4	5	6
8	9	1	2	3	4	5	6	7
9	1	2	3	4	5	6	7	8

JG10.388-1c

Object matrix

13	12
14	15
12	13

Figure 1: The Background Matrix and the Object Matrix.

Movement of the object

1	2	3	4	5	6	7	8	9
2	3	4	5	6	7	8	9	1
3	4	5	6	7	8	9	1	2
4	5	6	7	8	9	1	2	3
5	6	7	13	12	1	2	3	4
6	7	8	14	15	2	3	4	5
7	8	9	12	13	3	4	5	6
8	9	1	2	3	4	5	6	7
9	1	2	3	4	5	6	7	8

$S_q = 3.16$
$S = 0.61$

1	2	3	4	5	6	7	8	9
2	3	4	5	6	7	8	9	1
3	4	5	6	7	13	12	1	2
4	5	6	7	8	14	15	2	3
5	6	7	8	9	12	13	3	4
6	7	8	9	1	2	3	4	5
7	8	9	1	2	3	4	5	6
8	9	1	2	3	4	5	6	7
9	1	2	3	4	5	6	7	8

Movement of the background

1	2	3	4	5	6	7	8	9
2	3	4	5	6	7	8	9	1
3	4	5	6	7	8	9	1	2
4	5	6	7	8	9	1	2	3
5	6	7	13	12	1	2	3	4
6	7	8	14	15	2	3	4	5
7	8	9	12	13	3	4	5	6
8	9	1	2	3	4	5	6	7
9	1	2	3	4	5	6	7	8

$S_q = 3.99$
$S = 0.88$

1	2	3	4	5	6	7	8	9
2	3	4	5	6	7	8	9	1
3	4	5	6	7	8	9	1	2
4	5	6	7	8	9	1	2	3
5	6	7	13	12	1	2	3	4
6	7	8	14	15	2	3	4	5
7	8	9	12	13	3	4	5	6
8	9	1	2	3	4	5	6	7
9	1	2	3	4	5	6	7	8

JG10.388-2c

Figure 2: Analysis of the movement of the object and the movement of the background.

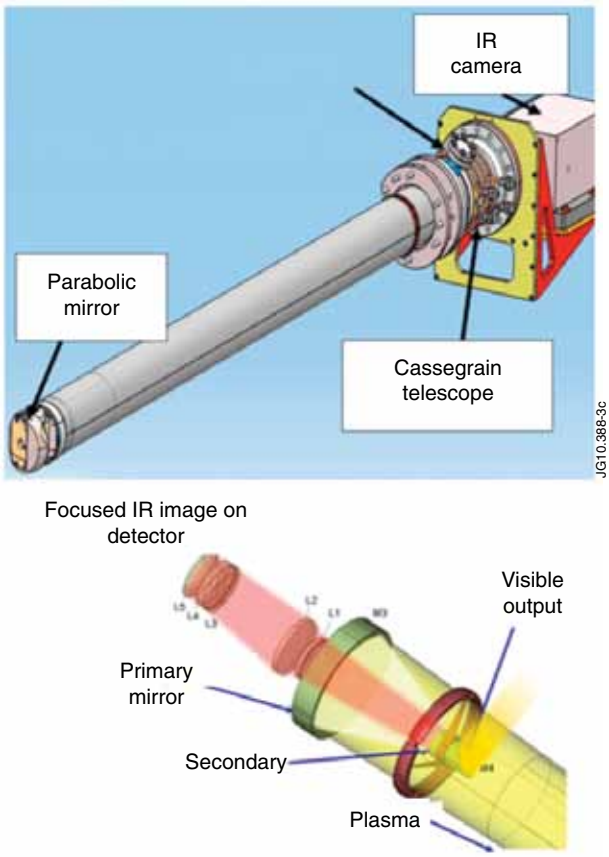

Figure 3: Top: the endoscope supporting the IR camera. Bottom: the Cassegrain configuration of the collection optics.

Figure 4: View of the torus taken with the IR wide angle camera, Pulse No: 66867, frame 115.

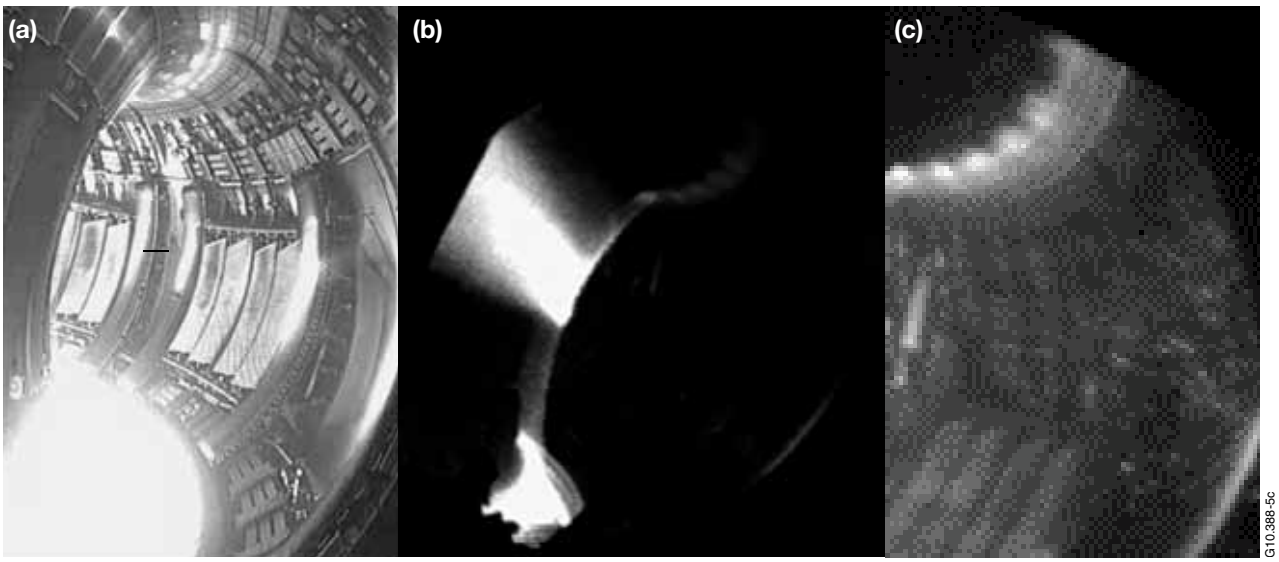

Figure 5: Example of an ELM producing flashes of light in various region of the vacuum vessel (5.a), a MARFE producing a band of emission along the inner wall on the high field side (5.b) and UFOs entering the plasma from the right of the field of view (5.c).

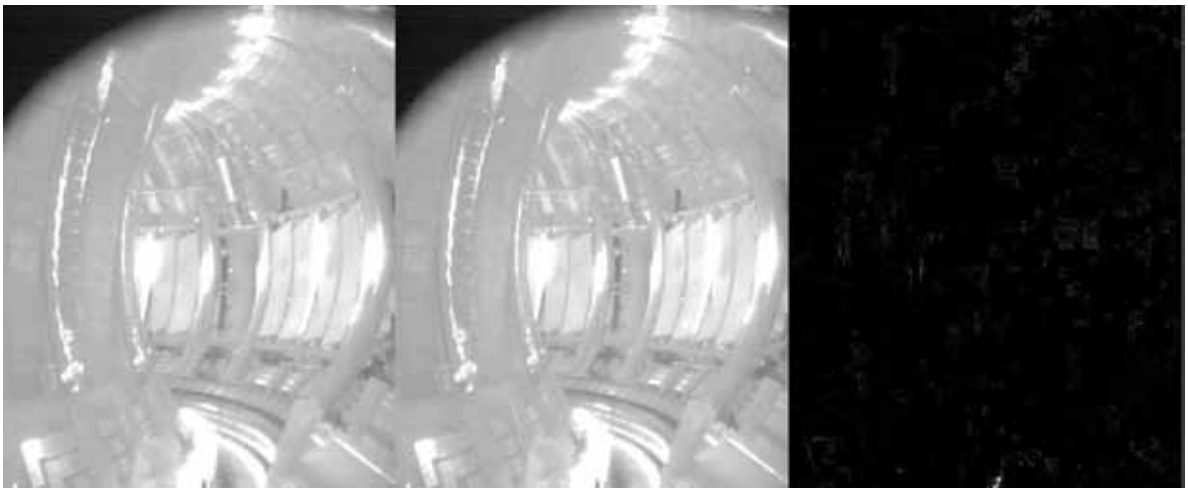

Two subsequent frames and their differences without vibration.

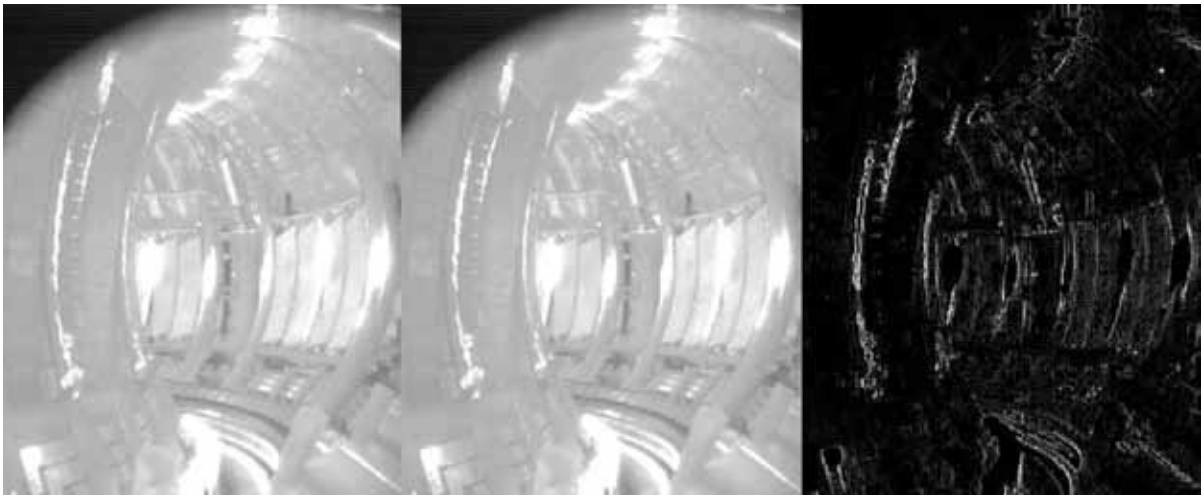

Two subsequent frames and their differences with vibration.

JG10.388-6c

Two subsequent frames and their differences without vibrations but with a MARFE

Figure 6: Example of the difference between two frames Top: a case without vibrations and without any motion of objects. Middle: a case of strong movement of the camera between the two subsequent frames but without any movement of objects within the field of view. The appearance of long range structures due to the movement of the background is very clear. Bottom: a case without vibrations but with a big object, a MARFE, moving within the field of view. Only short range structures appear in the differnce.

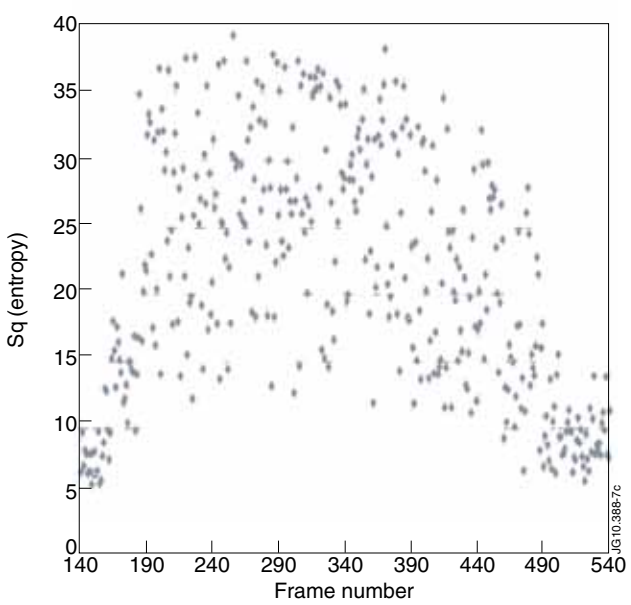

Figure 7: Evolution of the Sq entropy, as a function of the reference frame, for part of the video recorded by the wide angle IR camera for the Pulse No: 68815.

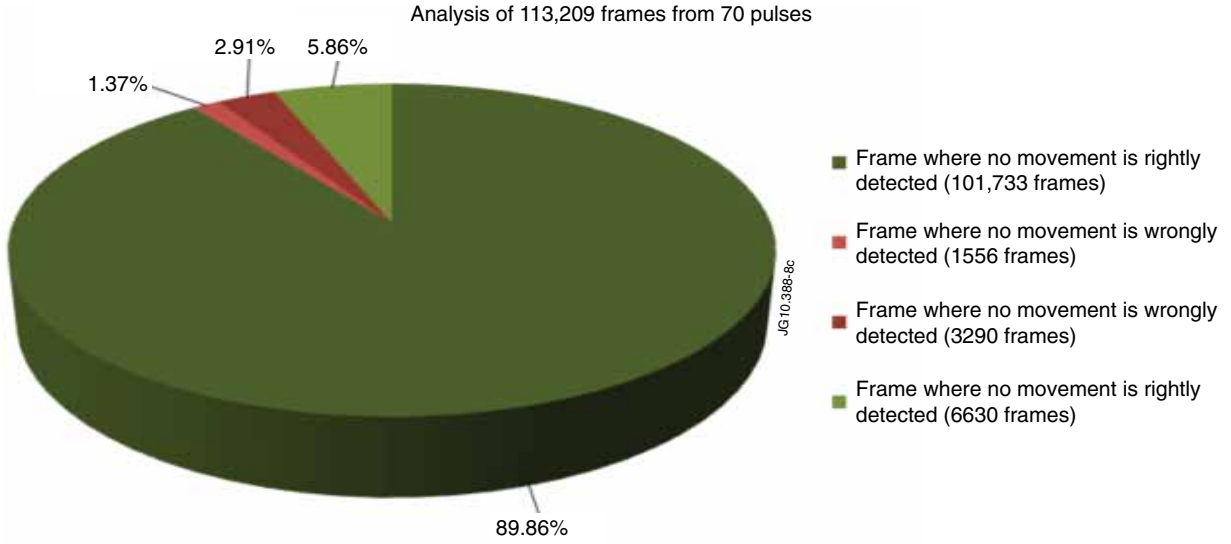

Figure 8: Result of the analysis of 70 videos and a total of 113,209 frames.

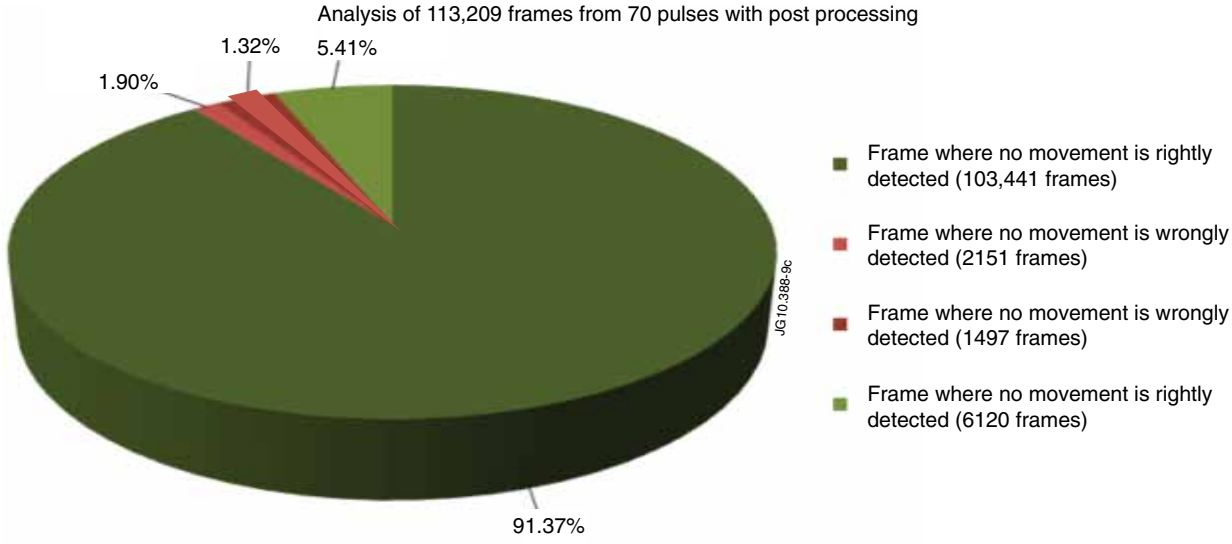

Figure 9: Result of the analysis of 70 videos and a total of 113,209 frames with post-processing.